Open Access Journal

Journal of Power Technologies 95 (2) (2015) 105–111

journal homepage:papers.itc.pw.edu.pl

Emission characteristics of a novel low NO_x burner fueled by hydrogen-rich mixtures with methane

Marcin Dutka[*,a], Mario Ditaranto[b], Terese Løvås[a]

[a]*Department of Energy and Process Engineering, Norwegian University of Science and Technology, Kolbjørn Hejes vei 1b, 7491 Trondheim, Norway*

[b]*SINTEF Energy Research, Sem Sælands vei 11, 7034 Trondheim, Norway*

Abstract

The use of hydrogen-rich fuels may be challenging for burner designers due to unique properties of hydrogen compared to conventional fuels such as natural gas. Burner retrofit may be required to use hydrogen-enriched fuels in combustion systems that are designed for natural gas combustion. This study aimed to experimentally investigate NO_x emissions from a novel low NO_x burner fueled by methane-hydrogen mixtures. The burner was tested in a cylindrical combustion chamber at atmospheric pressure. Burner thermal load of 25 kW (LHV) and air-fuel equivalence ratio of 1.15 were maintained throughout the experimental campaign. The influence of burner design parameters on NO_x emissions was tested for various fuel compositions using a statistically cognizant experimental design. The study revealed that shifting the burner head upstream can deliver NO_x emission reduction. In contrast, supplying fuel to the burner through secondary fuel ports increases NO_x emissions, particularly when the burner head is shifted upstream. The lowest predicted NO_x emissions from the burner are below 9 ppmvd at 3% of O_2 and 14 ppmvd at 3% of O_2 for 5% and 30% mass fraction of hydrogen in the fuel, respectively.

Keywords: low NO_x burner, hydrogen enrichment, nitrogen oxides, central composite design, bluff body

1. Introduction

The use of hydrogen-enriched fuels is one of the promising ways to significantly reduce carbon dioxide emissions from existing combustion systems. In addition, pollutant emissions such as carbon monoxide (CO), unburned hydrocarbons, and soot particles can be reduced by enriching conventional fuel with hydrogen. Therefore, hydrogen is considered the most promising future energy carrier.

However, this is challenging for burner designers. First, the high laminar flame speed of hydrogen-air mixtures leads to changes in the flame shape compared to the methane-air flame shape. As shown in Fig. 1, at the same equivalence ratio, the speed of a hydrogen–air flame is an order of magnitude higher than that of a pure methane-air flame. Under certain conditions, this may lead to the overheating of burner hardware and, consequently, burner damage. Second, the use of fuels containing hydrogen and hydrocarbons causes corresponding changes in NO_x emissions, which strongly depend on fuel composition, because the addition of hydrogen to hydrocarbon fuel increases adiabatic flame temperature. This temperature is a characteristic parameter of a fuel-oxidizer mixture and is correlated with laminar flame speed. Accordingly, the data in Fig. 1 also provide an overview of the increase in adiabatic flame temperature for various methane-hydrogen mixtures.

The main reason for the increase in NO_x emissions when hydrogen-enriched methane is used in a combustion system is the fact that the thermal NO_x formation mechanism that often dominates other NO_x formation mecha-

*Corresponding author
Email address: marcin.d.dutka@ntnu.no (Marcin Dutka[*,a])

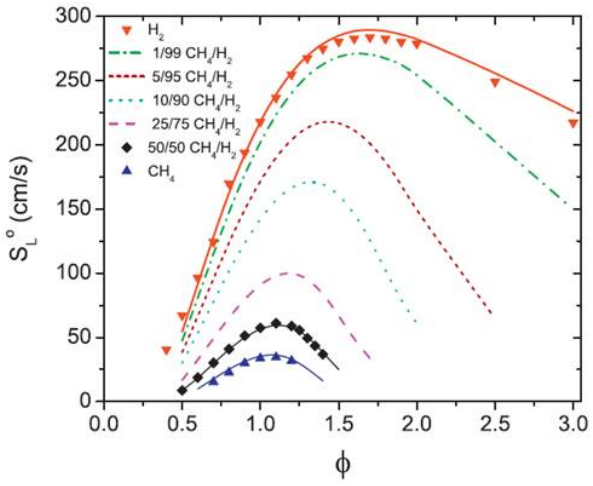

Figure 1: Laminar flame speed (S_L) of methane-hydrogen mixtures expressed by volume fraction at various equivalence ratios (ϕ) at 300 K and 1 atm in air [1]

nisms is strongly dependent on flame temperature. Therefore, to maintain NO_x emissions at acceptable levels, effective reduction of thermal NO_x from combustion systems using hydrogen-rich fuels can be of greater importance than from systems using conventional fuels. Moreover, NO_x emission characteristics may vary depending on burner design and fuel-air mixing.

An investigation of the effect of burner design parameters is required during burner development to ensure burner operation at the optimal settings for each fuel composition, as well as to determine emission performance and fuel flexibility capacity of the burner. Sometimes, burner retrofit may be required when planning to switch to hydrogen-enriched fuels in combustion systems designed for methane or natural gas combustion. Burner design should ensure safe, stable combustion and fulfillment of regulated pollutant emission standards.

Combined refinery gas consisting of streams originating from various process units within a refinery—for example, cracked gas, coking gas, reforming gas, fluid catalytic cracking (FCC) gas—contain only a few percent of hydrogen by volume. Other gases used in this industry that contain relatively significant amounts of hydrogen are pressure swing adsorption (PSA) tail gas and flexicoking waste gas. These gases contain approximately 20–30% of hydrogen by volume [2].

A novel partially premixed bluff body (PPBB) burner was considered for use in refinery fired heaters retrofitted for the combustion of hydrogen-enriched fuels [3]. NO_x emission performance of the burner was investigated by Dutka et al. [4]. However, experimental constraints did not allow for investigation of the effect of a wide range of burner design parameters on NO_x emissions. Furthermore, the experiment was designed to compare NO_x emissions from pure methane combustion with NO_x emissions from hydrogen-enriched methane combustion.

This led the authors to conduct an experimental campaign focused on testing another PPBB burner using hydrogen-rich methane-hydrogen mixtures and investigating the influence of its design parameters on NO_x emissions. In this study, the authors determine the emission characteristics of a PPBB burner fueled by methane enriched with hydrogen up to 77% by volume. The high-hydrogen concentration fuel mixtures tested in the experimental campaign are called hydrogen-rich fuels in this paper. The presented burner NO_x emission performance was determined based on emission measurement results which were obtained according to statistically cognizant experimental design, similar to that used by Dutka et al. [4]. This experimental approach allowed for minimization of experimental trials, lower experiment costs, and shorter experimental duration [4, 5].

2. Experimental methodology

Central composite design [6] (CCD) is an experimental design used in response surface methodology. This approach was described in detail by Dutka et al. [4], and only a brief description of the CCD technique is presented herein. Generally, CCD is used in statistically designed experiments to develop a second-order polynomial model, similar to the one given by Eq. 1 The model uses k factors $X_1 \ldots X_k$ to predict the investigated response y. The coefficients in the equation, namely, $\beta_1 \ldots \beta_k$, are determined by fitting a response surface to experimentally measured values using the least-squares method. ε is the error associated with the model, which is inevitable because it is impossible to perfectly fit a second-order polynomial curve to the measured dataset.

$$\begin{aligned} y = \beta_0 + \beta_1 X_1 + \beta_2 X_2 + \ldots + \beta_k X_k + \\ + \beta_{11} X_1^2 + \beta_{22} X_2^2 + \ldots + \beta_{kk} X_k^2 + \\ + \beta_{12} X_1 X_2 + \ldots + \beta_{k-1,k} X_{k-1} X_k + \varepsilon \end{aligned} \quad (1)$$

The coefficients need to be determined for each given system. For this purpose, one can use CCD, which strictly defines measurement points, i.e., combinations of levels of factors to be tested. It implies certain model prediction properties and affects variance of the predicted response. The points in Fig. 2 show a unique set of combinations of three factors tested in an experiment according to circumscribed CCD.

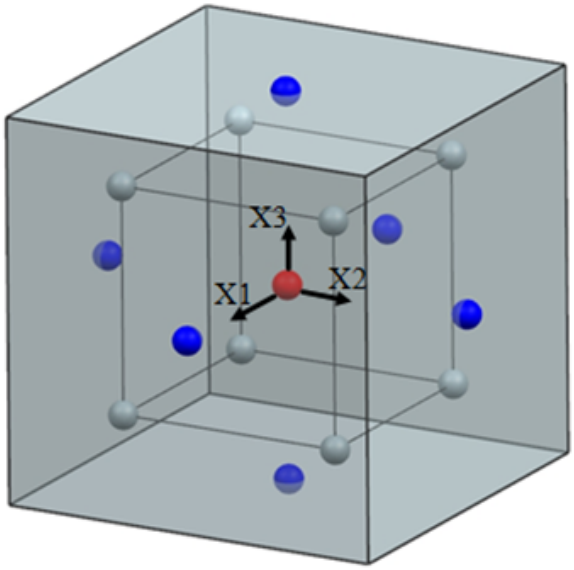

Figure 2: Schematic representation of circumscribed CCD for 3 factors: X1, X2, and X3 [4]

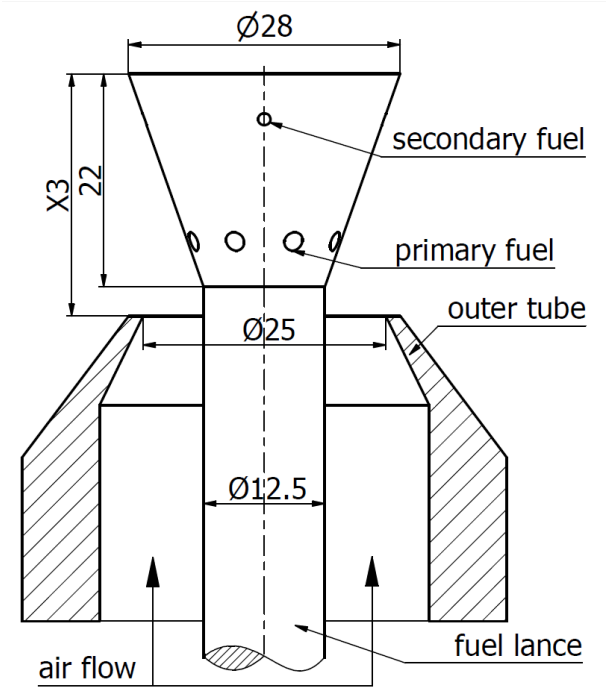

Figure 3: Schematic representation of PPBB burner used in experiments (dimensions in millimeters) [4]

In this design, factors were tested at five levels: -1, $-1/\alpha$, 0, $1/\alpha$, and 1, where α is defined by Eq. 2. Factor levels were normalized (or coded) so that -1 and 1 corresponded to the minimum and maximum values of the tested factor, respectively.

$$\alpha = \left(2^k\right)^{0,25} \tag{2}$$

Such an arrangement of points of the design ensures rotatability of the design, i.e., constant variance in response estimation at a specified distance around the center point where all factors are tested at level 0 in coded units [7]. Moreover, the arrangement restricts the experimenter's region of interest between -1 and 1 for each factor, so that the region can be graphically represented as a three-dimensional cube with a side length of 2 in coded units.

3. Experimental apparatus and approach

A PPBB burner, shown in Fig. 3, was used to experimentally investigate NO_x emissions from the combustion of hydrogen-rich mixtures with methane. The burner is similar but not identical to the burner used in the previous studies [4]. The only difference between these two burner designs is the fuel port diameter, with the redesigned burner exhibiting better flame stability owing to fuel port diameter modification.

A PPBB burner consists of a burner head, also called a lance, and an outer tube. Fuel is distributed from the lance in a cross-flow, relative to the flow of accelerated air, from the primary and secondary fuel ports. These ports are arranged around the lance. The mixture flows through the narrowest section of the air duct called the burner throat and fuel is partially premixed with air before entering the flame stabilization zone. The flame is stabilized behind the lance because of the recirculating wake structure formed in this region. Images of the flame are shown in Fig. 4.

The PPBB burner was mounted vertically in the cylindrical combustion chamber. The chamber height, outer diameter, and wall thickness were 1000, 360, and 5 mm, respectively. Heat loss from the chamber by natural convection and radiation to ambient conditions was estimated to be 40–48%.

All emission measurements were conducted at atmospheric pressure, constant burner thermal load of 25 kW (calculated based on LHV), and constant air-fuel equivalence ratio of 1.15. The sample for gas composition analysis was taken from the chamber outlet and delivered to a pre-calibrated Horiba PG-250 gas analyzer.

The experiment was designed according to the circumscribed rotatable CCD [6] for 3 factors. It entailed conducting measurements at 20 points, including 5 replicates of the center point of the design.

The following factors were investigated:

1. Hydrogen mass fraction in fuel (X1)
2. Secondary fuel fraction in fuel stream (X2)

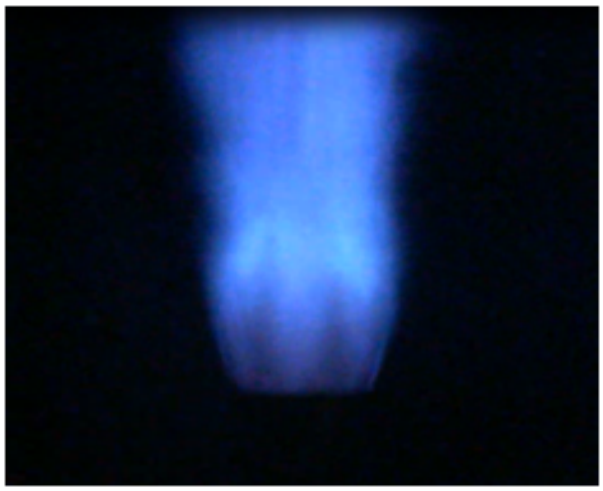

(a) CH_4 = 100%, H_2 = 0%

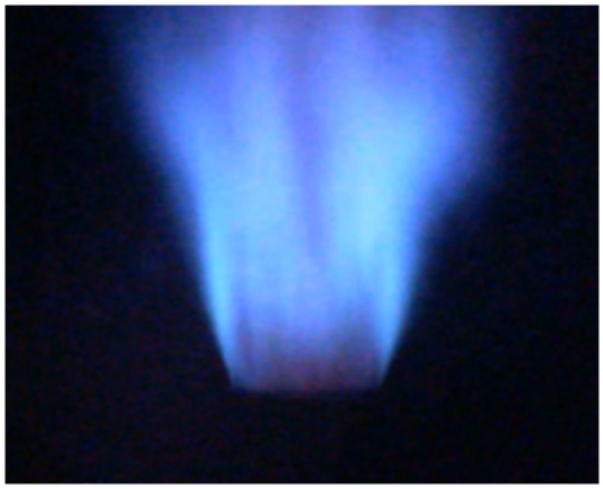

(b) CH_4 = 85%, H_2 = 15% (by mass)

Figure 4: Comparison of flame shape of pure methane-air flame [4] and hydrogen-enriched methane-air flame stabilized on the PPBB burner lance

3. Distance between the top surface of the lance and burner throat (X3) (shown in Fig. 3)

Each of these factors was tested at five levels to meet the condition of design rotatability. The air flow velocity at the burner throat (or the air outlet section) ranged from 22 to 36 m/s, depending mainly on the lance position. Detailed information about the ranges of the factors tested is given in Table 1.

4. Results and discussion

The experimental matrix showing the operating conditions for each experimental trial and the respective measured NO_x and CO emission values is presented in Table 2. Based on the NO_x emission measurements, an empirical correlation was developed by fitting a response surface to the measured NO_x emissions at points defined by the CCD. The model is defined by Eq. 3.

Table 1: Levels of factors tested in the experiment

Factor	Coded units				
	-1	$-1/\alpha$	0	$1/\alpha$	1
X1, %	5	10.07	17.5	24.93	30
X2, %	0	4.05	10	15.95	20
X3, mm	13	14.42	16.5	18.58	20

$$\begin{gathered} NOx = -31.271+ \\ +0.664X_1 + 2.534X_2 + 3.277X_3- \\ -0.01X_1^2 - 0.032X_2^2- \\ -0.09X_2X_3 \end{gathered} \tag{3}$$

Application of analysis of variance (ANOVA) [8] allowed for the removal of statistically insignificant terms at the 95% confidence level from the model and improved the model's prediction capability.

Standard error of the regression was estimated to be 0.92 mg/kWh. The coefficient of determination (R^2) [9] of the measured NO_x emissions and the emissions predicted by the model at the design points was 97.8%, while predictive power of the model estimated based on the predicted R^2 was 94.2%. The model was used to analyze the influence of the factors tested on NO_x emissions.

The contour plots presented in Figs. 5 and 6 show NO_x emissions for two of the three factors investigated during the experiment, while the third factor was kept constant. In all contour plots, NO_x emissions increase upon the addition of hydrogen to methane. This trend is observed across entire ranges of secondary fuel fraction and lance positions investigated in the experiment.

However, upon the addition of greater amounts of hydrogen to the methane-hydrogen mixture, the distance between the isolines of NO_x emissions increases with constant lance position and secondary fuel fraction. Therefore, for higher hydrogen concentrations in the fuel, NO_x emissions can be expected to increase at a slower pace within the investigated hydrogen proportion range. This may be ascribed to the low amount of carbon atoms in the fuel and, therefore, the diminished role of the prompt mechanism in NO_x formation with the addition of hydrogen to the fuel. Nevertheless, the thermal mechanism, which is affected by increased flame temperature, contributes more to NO_x formation and total NO_x emissions increase regardless of burner operation settings.

Table 2: Experimental matrix

Factor	X1 %	X2 %	X3 mm	NO_x ppmvd	CO ppmvd	NO_x mg/kWh	Predicted NO_x mg/kWh	Residual mg/kWh
1	10.07	4.05	14.42	13.9	1.5	27.0	26.07	1.0
2	24.93	4.05	14.42	15.9	0.1	29.1	30.50	-1.4
3	10.07	4.05	18.58	19.6	0.0	38.2	38.19	0.0
4	24.93	4.05	18.58	23.8	0.0	43.6	42.62	1.0
5	10.07	15.95	14.42	16.4	3.0	32.1	33.08	-1.0
6	24.93	15.95	14.42	20.2	0.0	36.9	37.51	-0.6
7	10.07	15.95	18.58	20.6	0.0	40.2	40.72	-0.5
8	24.93	15.95	18.58	24.9	0.0	45.5	45.15	0.4
9	5.00	10.00	16.50	16.6	6.3	33.3	33.08	0.2
10	30.00	10.00	16.50	22.7	0.4	40.7	40.53	0.2
11	17.50	10.00	13.00	16.3	0.8	30.7	30.14	0.6
12	17.50	10.00	20.00	24.2	0.0	45.6	46.75	-1.2
13	17.50	0.00	16.50	16.3	0.0	30.8	31.22	-0.5
14	17.50	20.00	16.50	21.3	0.0	40.1	39.24	0.9
15	17.50	10.00	16.50	20.1	0.0	38.0	38.44	-0.5
16	17.50	10.00	16.50	20.2	0.0	38.2	38.44	-0.3
17	17.50	10.00	16.50	20.5	0.0	38.6	38.44	0.2
18	17.50	10.00	16.50	20.9	0.0	39.5	38.44	1.0
19	17.50	10.00	16.50	20.1	0.0	37.9	38.44	-0.6
20	17.50	10.00	16.50	20.9	0.0	39.5	38.44	1.1

The strongest factor affecting NO_x emissions is the lance position. It affects air speed and flow pattern behind the lance. If fuel is provided to the burner using only primary fuel ports, shifting the lance toward the burner throat results in NO_x emission reduction from 37 mg/kWh to 14 mg/kWh for fuel containing 5% mass fraction of hydrogen. When the hydrogen mass fraction in the fuel reaches 30%, NO_x emissions can be reduced from 45 mg/kWh to 22 mg/kWh. It is important to note that NO_x emissions were measured at a lance position of 13 mm, because shifting the lance further toward the burner throat led to incomplete fuel combustion, manifested as CO emission. This effect was already observed at higher lance positions, as shown by Dutka et al. [4]. It was probably caused by the fact that at lower lance positions, fuel streams are entrained by high-velocity air and not all of the fuel flows into the combustion zone behind the lance or the residence time is not long enough for complete fuel combustion. However, this limitation of the lowest lance position was dictated by the symmetrical nature of CCD and, therefore, the symmetrical space of the design.

The adverse effect of shifting the lance toward the burner throat was not observed for fuels containing more hydrogen in their composition due to the high hydrogen diffusivity and high temperature in the combustion zone. Partly for this reason, namely, unacceptably high CO emission, fuel mixtures containing lower fractions of hydrogen were not tested in this study. Thus, the minimum hydrogen mass fraction was restricted to 5%.

When a certain portion of fuel was supplied to the burner using secondary fuel ports, NO_x emissions increased for all tested fuel compositions.

This is an interesting finding, because a similar effect of secondary fuel fraction was not observed in the tests performed earlier, where this parameter had negligible impact on NO_x emissions [4]. It can be explained by the fact that in this study, a wide range of secondary fuel fractions was tested. It is also important to note that, as shown in Fig. 6, the secondary fuel fraction affects NO_x emissions significantly at lower lance positions, and it does not influence NO_x emissions when the lance is shifted downstream. This explains why this factor could not be omitted from the model formulation, because it contributes significantly change in NO_x emissions within the tested factor ranges.

By modifying the distribution of fuel streams at the lowest tested lance position, NO_x emissions were reduced from 29 to 14 mg/kWh for fuel containing 5% mass fraction of hydrogen and from 36 to 22 mg/kWh for fuel con-

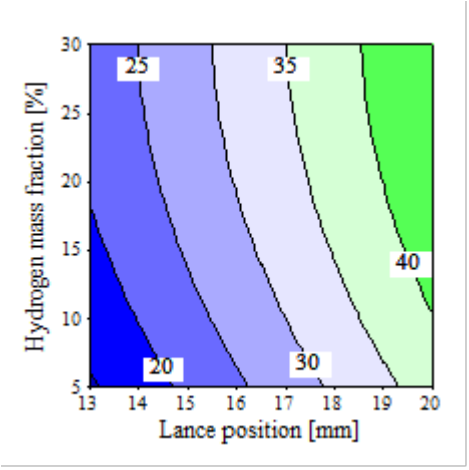

(a) X2 = 0%

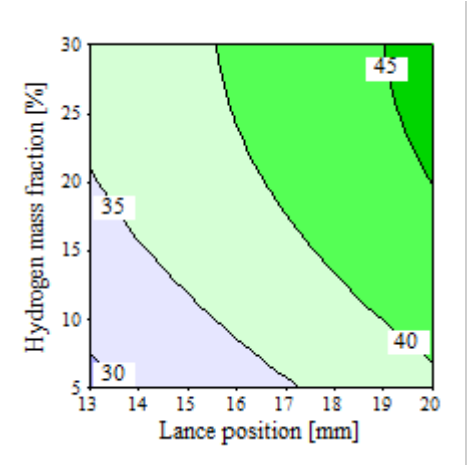

(b) X2 = 20%

Figure 5: Contours of NOx emissions in mg/kWh for various hydrogen mass fractions in fuel and lance positions with a constant secondary fuel fraction

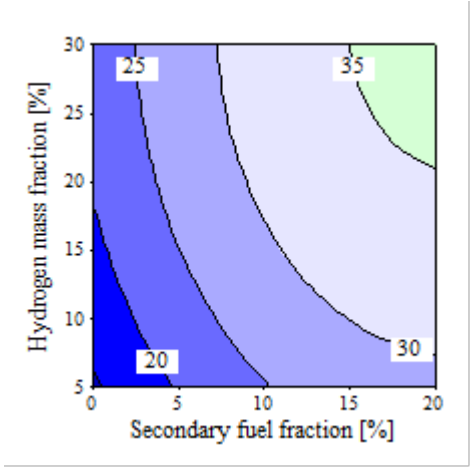

(a) X3 = 13 mm

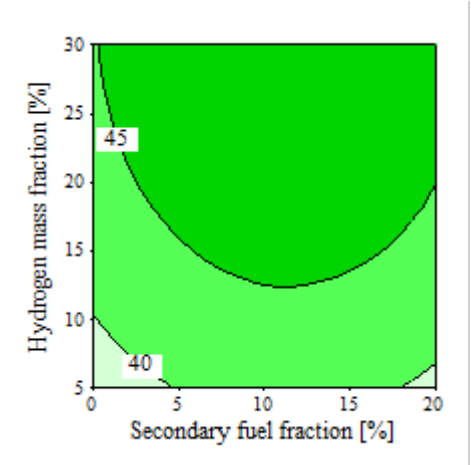

(b) X3 = 20 mm

Figure 6: Contours of NOx emissions in mg/kWh for various hydrogen mass fractions in the fuel and secondary fuel fractions with a constant lance position

taining 30% mass fraction of hydrogen. Moreover, it was observed that higher amounts of fuel provided through secondary fuel ports resulted in lower flame stability and under certain conditions in the case of hydrogen-lean fuel mixtures, flame extinction. This may be attributed to unacceptably high fuel concentration in the combustion zone, i.e., the region behind the lance, preventing flame stabilization.

NO_x emission values for various burner operation settings should be regarded as trends rather than exact values of NO_x emissions. In the circumscribed CCD, variance of the model is almost constant over distances equal to 1 in coded units from the center point. However, the variance increases significantly at greater distances from the center point, which should be taken into account when predicting NO_x emissions at values of all factors equal to –1 or 1 in coded units. Statistical evaluation of confidence intervals or prediction intervals is required to assess possible deviation from the values predicted by the model.

Therefore, assuming that the relationships described by the model are valid even far from the center point of the design, i.e., at a secondary fuel fraction equal to 0% and lance position of 13 mm from the burner throat, the PPBB burner may offer the possibility of firing hydrogen and methane mixtures with average NO_x emission lower than 17.5 mg/kWh for mixtures containing 5% mass fraction of hydrogen and lower than 25 mg/kWh for mixtures containing 30% mass fraction of hydrogen. These values are the upper limits of the 95% confidence intervals associated with the model and the most promising burner operation settings.

5. Conclusions

On the basis of a combined response surface methodology and CCD, a burner study was performed with the least number of possible measuring points. Three factors were investigated. It was found that NO_x emissions are affected by hydrogen concentration in a methane-hydrogen mixture. The PPBB burner allows for the minimization of NO_x emissions when fuel is supplied through primary fuel ports only, and the lance is located close to the burner throat. The minimum predicted NO_x emissions were lower than 17.5 and 25 mg/kWh for mixtures containing 5% and 30% mass fractions of hydrogen, respectively. It can be expected that the PPBB burner allows for the combustion of methane-hydrogen mixtures with NO_x emissions lower than 9 ppmvd at 3% O_2 for 5% mass fraction of hydrogen and below 14 ppmvd at 3% O_2 for mixtures containing 30% mass fraction of hydrogen. These NO_x emission levels are very promising when compared to the minimum NO_x emissions (15 ppmvd at 3% O_2) achieved with low and ultra-low NO_x burners for refinery fuel gas combustion, as listed in [10]. The results presented in this study form part of on-going research activity focused on burner testing under various operating conditions and burner scale-up to industrial size.

Acknowledgments

This publication was produced with support from the BIGCCS Centre, performed under the Norwegian research program Centers for Environment-friendly Energy Research (FME). The authors acknowledge the following partners for their contributions: ConocoPhillips, Gassco, Shell, Statoil, TOTAL, GDF SUEZ and the Research Council of Norway (193816/S60).

References

[1] N. Donohoe, A. Heufer, W. K. Metcalfe, H. J. Curran, M. L. Davis, O. Mathieu, D. Plichta, A. Morones, E. L. Petersen, F. Güthe, Ignition delay times, laminar flame speeds, and mechanism validation for natural gas/hydrogen blends at elevated pressures, Combustion and Flame 161 (6) (2014) 1432–1443.

[2] J. Ackland, J. White, R. Waibel, The John Zink Hamworthy Combustion Handbook, Second Edition, Industrial Combustion, CRC Press, 2012, Ch. Fuels, pp. 45–77, 3. doi:10.1201/b12975-4.
URL http://dx.doi.org/10.1201/b12975-4

[3] M. Ditaranto, R. Anantharaman, T. Weydahl, Performance and NOx emissions of refinery fired heaters retrofitted to hydrogen combustion, Energy Procedia 37 (2013) 7214–7220.

[4] M. Dutka, M. Ditaranto, T. Løvås, Application of a central composite design for the study of NOx emission performance of a low NOx burner, Energies 8 (5) (2015) 3606–3627.

[5] P. Bělohradskỳ, V. Kermes, Experimental study on NOx formation in gas-staged burner based on the design of experiments, Chem. Eng. Trans 29 (2012) 79–84.

[6] G. Box, K. Wilson, On the experimental attainment of optimum conditions, Journal of the Royal Statistical Society, ser. B (Methodological) 13 (1951) 1–45.

[7] G.E.P. Box, J.S. Hunter, W.G. Hunter, Statistics for Experimenters: Design, Innovation, and Discovery; Wiley-Interscience: Hoboken, NJ, 2005; pp 47, 455.

[8] C. P. Doncaster, A. J. Davey, Analysis of variance and covariance: how to choose and construct models for the life sciences, Cambridge University Press, 2007.

[9] R. L. Mason, R. F. Gunst, J. L. Hess, Statistical design and analysis of experiments: with applications to engineering and science, 2nd Edition, Vol. 474, John Wiley & Sons, New York, 2003.

[10] European Commission, IPPC Reference Document on Best Available Techniques for Mineral Oil and Gas Refineries, 2003.